Deployment Dynamics of Composite Booms with Integral Slotted Hinges

H.M.Y.C. Mallikarachchi*
University of Cambridge, Cambridge CB2 1PZ, U.K.

S. Pellegrino†
California Institute of Technology, Pasadena, CA 91125

This paper considers a lightweight boom with an integral hinge consisting of a thin-walled tube made of carbon fibre reinforced plastic with two longitudinal slots. The dynamic deployment of this boom is studied both experimentally and by means of detailed finite-element simulations. The deployment of the boom can be divided into three phases: deployment; incomplete latching, buckling of the tape springs and large rotation of the boom; and vibration of the boom in latched configuration. The simulations show that the most critical phase is the second one, as the highest strains in both the fibres and the matrix occur at this stage. Through the simulations it is found that the deployment of the particular boom design studied in this paper is quite sensitive to the details of the gravity offload system.

I. Introduction and Background

The aim of this research is to develop and validate modelling techniques to simulate the dynamic deployment behaviour of stored energy deployable structures made of composite materials. Large space structures of this type have several advantages over conventional structures with mechanical joints. They have already been used for a number of missions and a range of structural architectures based on the same approach is currently being considered for new applications. Their lightness, lower cost —because of a small number of component parts— and lack of frictional effects during deployment are distinctive advantages.

The deployment schemes that have been considered so far envisage the release of all constraints on the structure, to allow the structure to dynamically deploy and self-latch. However this behaviour needs to be fully understood and optimized as severe dynamic effects at the end of deployment could damage the structure and yet a slow, highly damped deployment may end without ever achieving the fully deployed configuration. Achieving a balance between these effects is challenging, as demonstrated by the large amount of testing and simulation that was required to achieve the successful deployment of the MARSIS booms.[1]

A self-motorized deployment mechanism introduced by Boesch et al.[2] incorporates four pairs of tape springs in a row, each with the concave side facing inwards. Thus the tapes in each pair are bent one in an equal sense, i.e. with longitudinal curvature in the same sense as the transverse curvature of the tape, and on in an opposite sense; this configuration which a high latching moment and hence a highly repeatable deployed configuration. However, depending on the amount of strain energy stored in the folded hinge and the maximum moment that it can carry without folding, the hinge may fail to properly latch the first time that it reaches the fully deployed configuration and, due to an excessive amount of kinetic energy, it may continue through the deployed configuration and fold in the opposite sense the tape spring that was originally bent in the equal sense. This process involves buckling of this tape spring and may cause permanent damage.

In this paper we consider a simple foldable structure made of linear-elastic material that poses many of the challenges that will be encountered also in larger structures, Figure 1. This particular example is itself

*Research Student, Department of Engineering, Trumpington Street, Cambridge CB2 1PZ, U.K. Currently on leave at California Institute of Technology

†Professor of Aeronautics and Civil Engineering, Graduate Aerospace Laboratories, 1200 East California Boulevard, Mail Code 301-46, Fellow AIAA. e-mail: sergiop@caltech.edu

of significant practical interest: it is a lightweight boom with an integral hinge that consists of a thin-walled tube made of carbon fibre reinforced plastic with two longitudinal slots with round ends. A variant of this hinge design, with three slots, was considered by Yee and Pellegrino;[3] also each folding section of the MARSIS booms had in fact an integral hinge.

Figure 1: Tube hinge: deployed, partially folded and fully folded.

Recently, we have studied the folding and quasi-static deployment of this tube hinge by means of numerical simulations that were verified experimentally.[4,5] The simulations were carried out with ABAQUS/Explicit commercial finite element package.[6] The tube hinge was modelled with four-node fully integrated shell elements and the ABD stiffness matrix for the thin laminate was obtained from a separate analysis based on the homogenization technique introduced by Kueh and Pellegrino for single-ply triaxial weave;[7] each tow in the representative unit cell was modeled as a linear-elastic solid with properties derived from the rule of mixtures and periodic boundary conditions were applied. Then the components of the ABD matrix were computed with Virtual Work, after carrying out six separate ABAQUS/Standard analyses, each corresponding to a unit amplitude of the six deformation variables, in-plane strains and out-of-plane curvatures.

The folding simulation mimicked the procedure to fold a hinge in practice. The hinge was first pinched in the middle and then rotated to the fully folded configuration. The deployment simulation consisted in rotating back the tube hinge under predefined equal end moment constraints until it reached the fully deployed configuration. The energy variation was monitored during the entire simulation and it was assumed that quasi-static behaviour had been achieved when the kinetic to internal energy ratio was less than 1%. Furthermore, the accuracy of the results was guarantied by ensuring that the difference between the work done and the summation of internal energy, kinetic energy and viscous dissipation, called energy balance in ABAQUS/Explicit was negligibly small. Figure 2 shows the moment-rotation relationship during quasi-static deployment for the particular tube hinge that was investigated.

To validate these results, a quasi-static deployment experiment was carried out with an apparatus that measures the end moments corresponding to any imposed set of end rotations. Good quantitative agreement was obtained between the moment-rotation relationship from the simulation and the measured one, with excellent correlation between predicted and observed deformed configurations of the tube hinge.

The present paper takes this earlier work to its next step. The same tube hinge is connected to a thin-walled, lightweight tube and the deployment dynamics and self-latching of this deployable structure are investigated by experiment and simulation. The layout of this paper is as follows. Section II describes the boom used for this research and Section III presents the deployment experiment. Section IV and V presents the simulation technique and its results. Section VI compares the experiments and the simulations and Section VII concludes the paper.

II. Construction of Test Boom

The folding section of the boom was 360 mm long, 0.2 mm thick and with internal diameter of 38 mm. It was made by laying two plies of plain-weave carbon fibre fabric (1k tows of T300 fibres) impregnated with HexPly 913 epoxy resin on a 38 mm diameter steel tube sprayed with PTFE release agent. The weave directions were at 45 deg to the axis of the tube. The fabric was wrapped in PTFE release film and was inserted into a heat-shrinking sleeve. Then the tube was cured under vacuum for one hour at 125°C and 600 kPa. After cooling, the steel tube was pulled out and two 140 mm long and 30 mm wide diametrically opposite parallel slots were cut with a Dremel 400 XPR high speed rotary tool. These cuts left two 25 mm

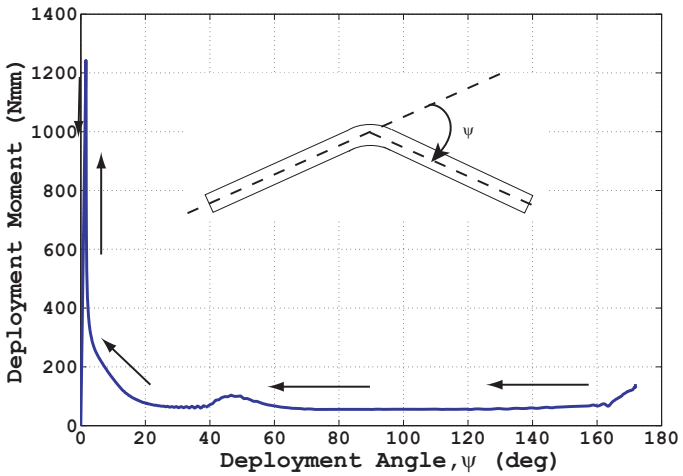

Figure 2: Predicted moment-rotation relationship for quasi-static deployment.

wide and 110 mm long, longitudinally straight tape springs with transverse radius of curvature of 19 mm, Figure 1.

This tube hinge was then connected to an Aluminium-alloy tube with an outer diameter of 38 mm and thickness of 0.9 mm. The connection was made by inserting the Aluminium tube into the tube hinge to provide a 25 mm overlap which was wrapped with electrical insulation tape and tightened with a hose clamp. The complete structure was 1025 mm long including the 1000 mm long boom and an additional length of 25 mm to provide a connection at the root of the boom, Figure 3.

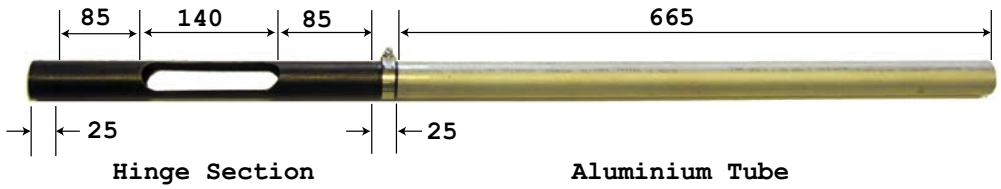

Figure 3: Complete boom (lengths in mm).

III. Deployment Tests

These tests were carried out on a rig that provided a single-point offload through a string attached to the outer surface of a tube, at a point directly above the centre of gravity of the Aluminium-alloy tube. The other end of the string was run through a pulley located at a height of 4150 mm, directly above the centre of the tube hinge. This constraint allowed the boom to only move in a horizontal plane. Figure 4 shows the experimental setup.

The root end of the boom was slid onto a 37.8 mm diameter 25 mm long solid Aluminium-alloy cylindrical fitting wrapped with thread sealing tape. A 6 mm thick sheet of rubber was wrapped around the tube and clamped with a hose clamp. The Aluminium cylinder was attached to a massive steel structure which provided a fixed end condition for the boom.

A Phantom V12.1 high speed camera was held directly above the folding part of the boom; its field of view included the folding part of the boom, up to the hose clamp. A second video camera was used to get an overall view of the deployment. A sheet of white paper with black lines at 5 deg angles provided a horizontal background from which the deployment angle could be measured.

First the boom was folded 45 deg and then released while recording the deployment with the high speed

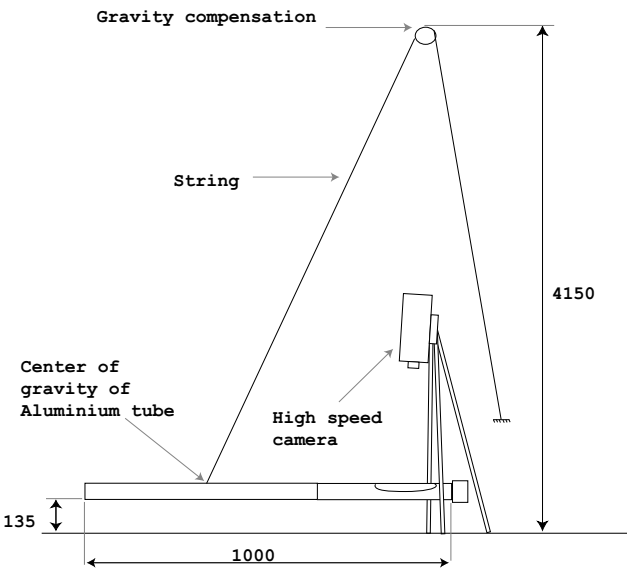

Figure 4: Experimental setup (units: mm).

camera at a rate of 300 frames per second. Figure 5 shows a series of images obtained from this experiment. The deployment history of the boom was derived by measuring the deployment angle from one frame out of every 25 frames (0.0083 s) using a specially written Matlab program that computes the angle between two lines manually drawn by an operator. Each picture was loaded to the background and the two lines were aligned with the boom and the 0 deg line on the white background sheet. The angle-time relationship obtained thus is plotted in Figure 6.

The same procedure was repeated after replacing the composite tube hinge with a second one, nominally identical to the first. Similar tests were carried out on both hinges after they were folded 90 deg. Figure 7 shows a series of images from this second test and a representative angle-time relationship is shown in Figure 8.

Consider, for example, Figure 6. The dynamic response of the boom can be generally divided into three phases: main deployment, incomplete latching and rotation of the boom beyond the fully deployed configuration (this may occur several times, see Figure 8) and final, small amplitude vibration of the deployed boom. Note that in these plots the value of the deployment angle is defined as 0 deg in the fully deployed configuration and positive in the folded configuration. The deployment phase lasted 0.96 s and 1.45 s, respectively, when the boom was folded 45 deg and 90 deg. The second phase, involving large rotations of the boom coupled with buckling of the tape springs, lasted 1.2 s with a maximum overshoot of 17 deg and 3.1 s with a maximum overshoot of 45 deg, respectively. The final variation continued for about 20 s in each case.

It should be noted that, although helpful in describing the deployment behaviour, the deployment angle does not fully identify the configuration of the boom. For example, the deployment angle may be zero with the boom not in the fully deployed configuration, as shown in Figure 9.

IV. Deployment Simulations

The finite element commercial software ABAQUS/Explicit was used for the deployment simulations. ABAQUS/Explicit is a tool that integrates the equations of motion for one node at a time and iterates through the whole structure using very small time steps. A key advantage of this approach for the present study is that it avoids any numerical difficulties associated with singularities in the stiffness matrix, which would occur in a standard, implicit solution. However, there are also several challenges that have to be overcome in order to obtain accurate results with this approach in problems that involve relatively long time scales, such as the present one. More details can be found in our previous paper.[5]

The complete model of the boom consisted of 2170 nodes and 2072 four node fully integrated shell

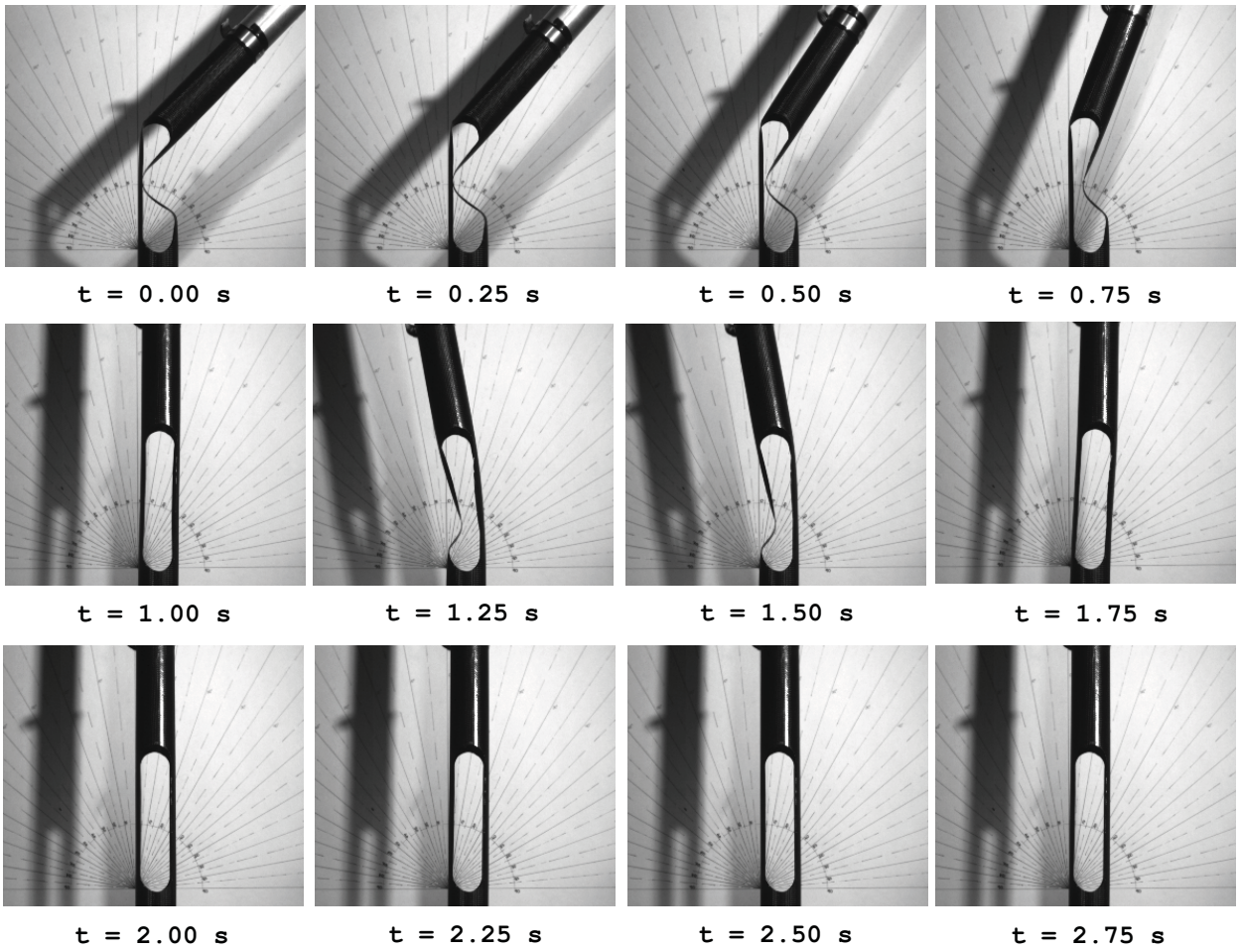

Figure 5: Photos taken during deployment of boom folded 45 deg.

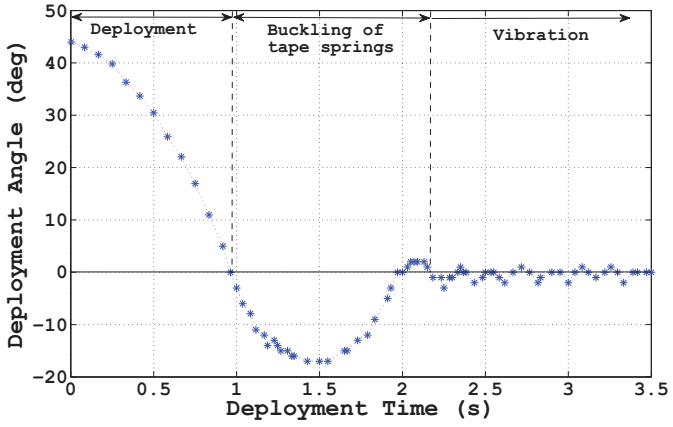

Figure 6: Angle vs. time relationship for boom folded 45 deg.

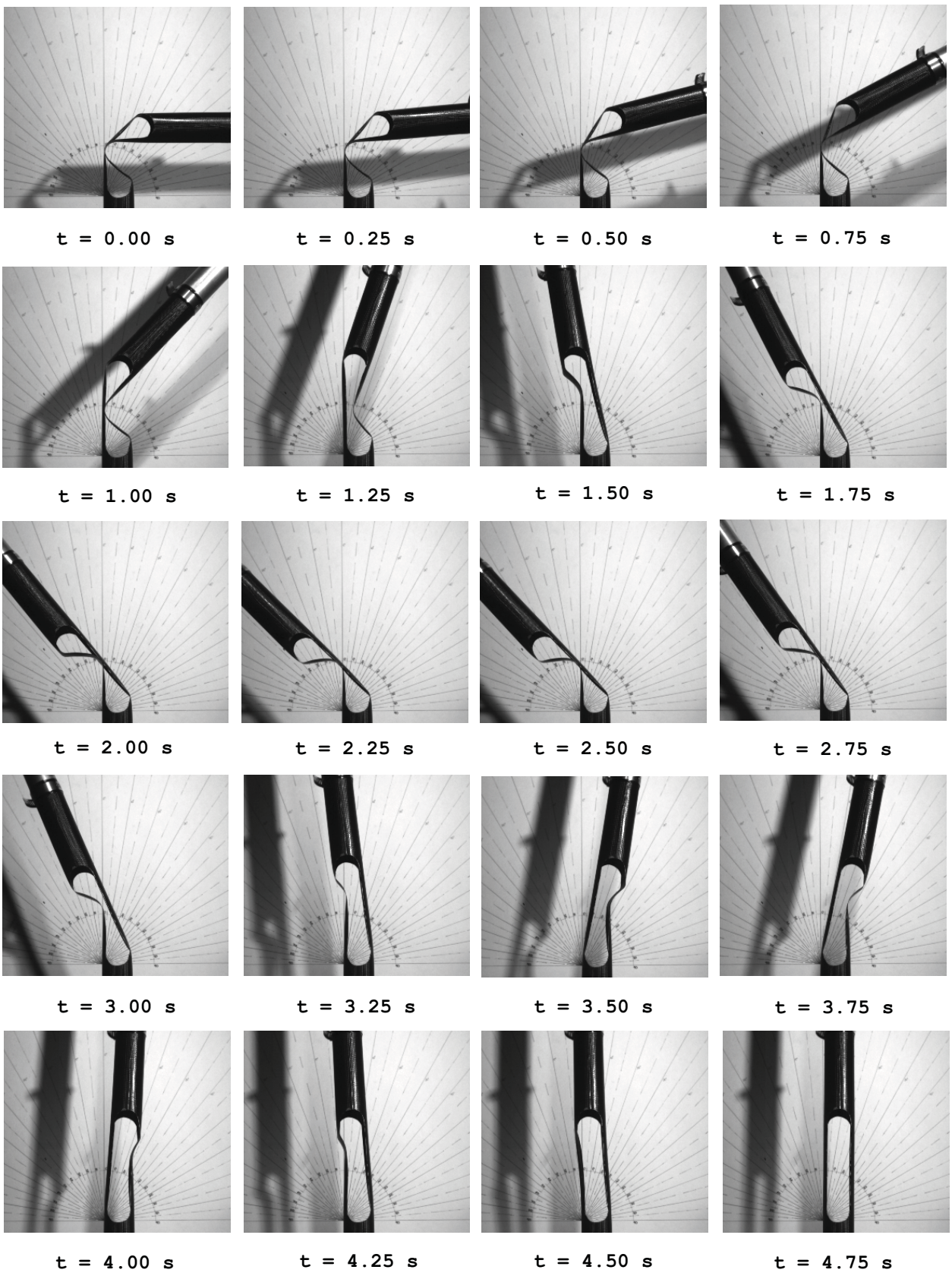

Figure 7: Photos taken during deployment of boom folded 90 deg.

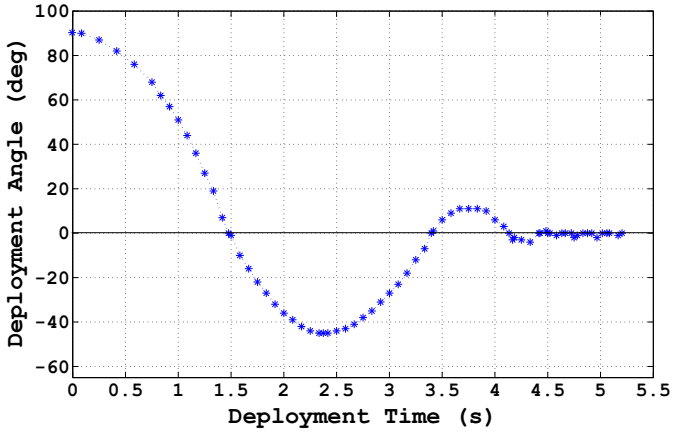

Figure 8: Angle vs. time relationship for boom folded 90 deg.

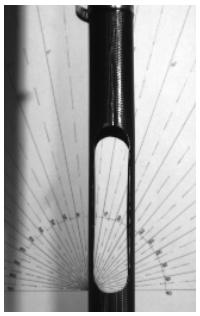

(a) Fully deployed configuration

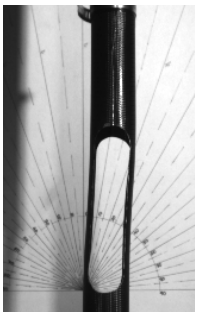

(b) Hinge sheared to the right

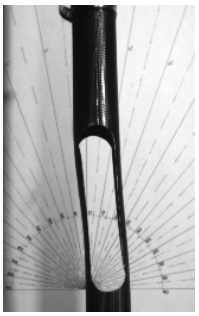

(c) Hinge sheared to the left

Figure 9: Different configurations of hinge with a zero deployment angle.

Region	Mass distribution
$0 < z < 322.5$ mm	318 g/m^2
$z = 322.5$ mm	25.79 g
$322.5 < z < 1000$ mm	2400 g/m^2

Table 1: Mass distribution of the finite element model

elements (S4). The mesh over the hinge region of the boom was finer, to capture the details of the complex deformation that occurs in this region. The material properties of the tube hinge were provided in the form of the ABD matrix[5] using the command **Shell General Section*. The material properties of the Aluminium tube were defined as isotropic with Young's modulus of 70 GPa and Poisson's ratio of 0.33. The additional mass of the connectors and overlap region was distributed over the nodes located at the corresponding cross-section. A full breakdown of the mass distribution is presented in Table 1.

The Aluminium tube is much stiffer than the tube hinge, hence it was modelled as a rigid body for computational efficiency. The fixed end condition at the end of the boom was defined by attaching the boom to a rigid ring. These two rigid bodies were connected to reference nodes A and B respectively, Figure 10. The reference node B was fixed by restraining all six degrees of freedom. The reference node A was restrained against translation in the x-direction and against rotations about the y and z axes to maintain symmetry during the folding simulation.

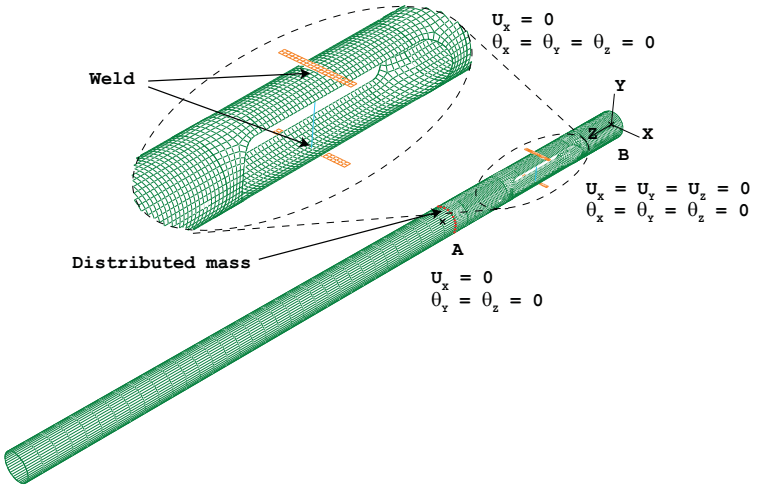

Figure 10: Finite element model of boom.

The first part of the simulation generates the folded configuration of the boom. The detailed sequence of steps that achieve this configuration is less important than the final folded configuration itself, provided that the kinetic energy in the folded configuration is sufficiently small. Because the hinge has much higher bending stiffness in the fully deployed configuration, the folding process was started by slightly pinching the hinge in the middle. This was done by defining two rigid plates, each consisting of a series of rigid bodies attached to a reference node. The two reference nodes were restrained to the y-z plane and were connected by a vertical beam element which was subjected to a thermal contraction. The connections between the beam element and the rigid plates were modelled as fixed connections using CONN3D2 elements and *Weld* connector sections.

The simulation involves several contact surfaces, as different parts of the boom come into contact with each other and also the rigid plates come into contact with the boom. The **General Contact* feature was used to simulate this behaviour, with the setting *Contact Inclusions, All Exterior* to define potential contact between all surfaces.

At the beginning of the folding simulation the beam element connecting the two rigid plates was shortened by decreasing its temperature and so the hinge was pinched as shown in Figure 11a and 11b. The next part

of the simulation involved rotating the reference node A in order to rotate the tube hinge. Node A was rotated through 45 deg about the x-axis over a period of 0.8 s; the accelerations were minimized by defining the rotation as a fifth-order polynomial function of time (*Smooth Step* in ABAQUS/Explicit). During the folding simulation a viscous pressure load was applied over the entire surface of the boom; the value of this pressure was defined by a pressure coefficient equal to 2×10^{-4} the density times the dilatational wave speed through the material, ρc_d, and the dimensionless linear bulk viscosity factor was set to zero.[5]

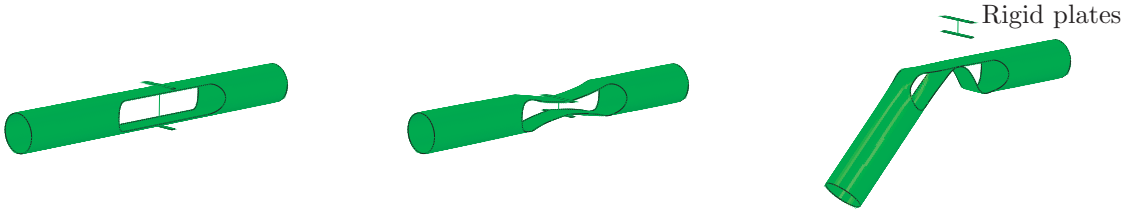

(a) Undeformed configuration (b) Pinching (c) Final folded configuration

Figure 11: Stages of folding simulation

At the end of the folding sequence, an additional step lasting 0.2 s was carried out with the viscous pressure load set 100 times higher, in order to quickly damp out any remaining kinetic energy while maintaining the reference node A stationary. This decreased the kinetic energy of the boom to practically zero, see Figure 12a, and hence achieved the fully folded static configuration. Contact between the plates used to pinch the boom and the boom was disabled at the beginning of this balancing step in order to avoid spurious interferences. Figure 11c shows the final folded configuration of the hinge.

This analysis had set up the boom in its folded configuration and hence ready for the deployment analysis. The viscous pressure coefficient was then set to zero because the viscous pressure tends to overdamp the dynamic response of the boom, however the linear bulk viscosity factor was set to 0.10. Deployment was triggered by releasing all constraints on the reference node A and by computing the response of the structure over a specified period of time, 4.0 s and 6.0 s for the boom with 45 deg and 90 deg folds, respectively. Unlike the folding simulation, where the simulation time had no physical meaning but was simply chosen such that the kinetic energy would never be too high, in the deployment analysis the simulation time is the actual time over which the motion occurs.

Figure 12b shows the energy variation during the deployment simulation. The peaks in the kinetic energy plot mark the instances when the boom achieves its fully deployed configuration. The variation in the viscous dissipation shows that most energy dissipation occurs after the deployment phase when the tape springs buckle. Note that the energy balance term (defined as the sum of internal energy, kinetic energy and viscous dissipation, minus the external work done) remains fairly constant during both rotation and deployment stages, which indicates that the simulation is free of major instabilities.[8] Also note that the increase of energy balance when the hinge is pinched, see Figure 12a, is due to the thermal energy associate with the decrease in the temperature of the beam element connecting the two rigid plates.

In the simulations described above zero-gravity conditions were assumed. A new set of simulations were carried out for another model that took into account gravity effects on the boom and also included the offload system. This was done by introducing a single 4161 mm long beam element with a Young's modulus of 8.96 GPa to model the cable. This beam was connected to the center of gravity of the Aluminium tube and to a fixed point with coordinates (4150 mm, 0, 155 mm).

V. Simulation Results

Figure 13 shows the variation of the deployment angle for a boom that is initially folded 45 deg, for zero-gravity conditions. This was obtained by recording the rotation of reference node A about the x-axis at every millisecond. The first part of the simulation, lasting about 0.93 s, shows a monotonic decrease of the deployment angle from 45 deg to 0 deg. Then the boom overshoots the fully deployed configuration several times, reacing a maximum angle of 20.5 deg. Finally, it remains locked in the fully deployed configuration but oscillates with an approximate amplitude of 1 deg at a period of about 0.18 s. This is a typical result from the simulations, more results are presented in Section VI.

In addition to predicting the overall deployment behaviour the simulation allows us to determine the

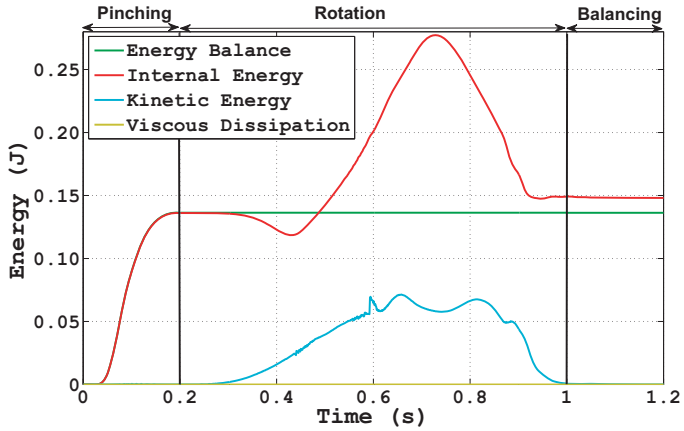

(a) Folding simulation

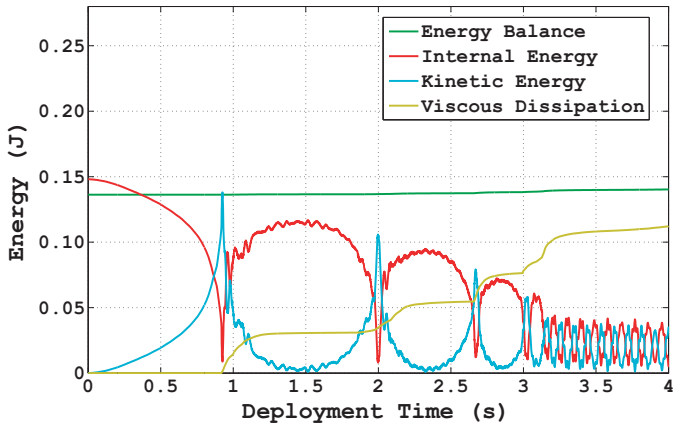

(b) Deployment simulation

Figure 12: Energy variation for 45 deg, zero-gravity simulation

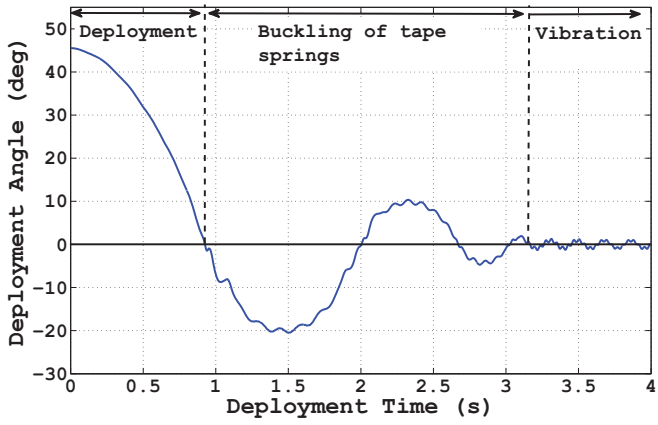

Figure 13: Zero-gravity simulation results for boom initially folded 45 deg.

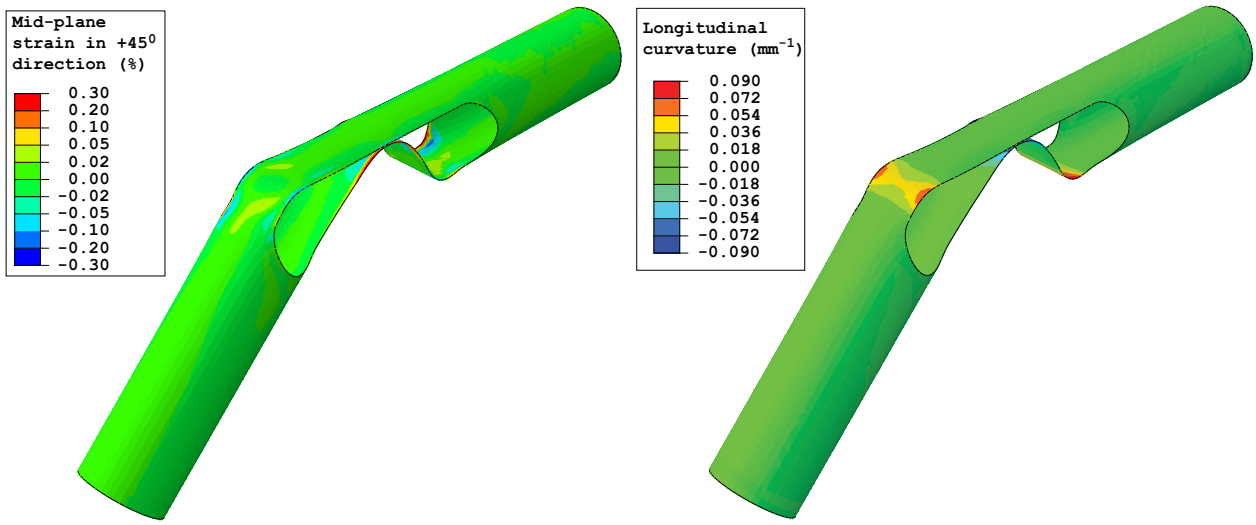

(a) Mid-plane strains in fibre direction

(b) Longitudinal curvature

Figure 14: Strains in 45 deg folded configuration.

safety margin of the structure. For example, a detailed analysis will be presented for the boom folded 45 deg, using a finer mesh with 6066 nodes and 5896 shell elements.

Figure 14 shows the mid-plane strain variation in the +45 deg direction as well as the longitudinal curvature in the fully folded configuration for this particular case. The margin of safety against fibre failure can be evaluated from the maximum strain failure criterion, where the maximum fibre strain is obtained by combining the structural boom model with the micromechanics material model for plain weave composites presented in Reference.[5] In the present case it is difficult to predict which configuration is the most critical because, in addition to the fully folded configuration, high strains may occur also during the latching phase. Hence, all configurations of the boom were analysed and the five configurations with the largest mid-plane strain (in absolute value) in the ±45 direction were selected. For each of these configuration, two critical locations were selected based on the value of both mid-plane strains and curvatures. Figure 15 shows the critical regions that were identified.

Next, to avoid numerical singularities in the strain distribution, the strain and curvature components near each critical location were compared to the maximum value and in cases where the maximum was over 30% than the average value, the second highest value was selected. Table 2 shows the strain and curvature components obtained through this process. Finally these components were introduced into the repeating unit cell model and the maximum fibre strain and matrix strain were computed from a detailed finite element analysis of the unit cell, see.[5] A total of ten different analyses of the periodic cell had to be carried out. The results of these analyses are presented in Table 3 which shows the maximum fibre and matrix strain at each critical location.

Location	1	2	3	4	5	6	7	8	9	10
Strain at +45° (%)	0.26	0.02	-0.12	0.20	0.17	-0.12	0.28	-0.14	0.29	-0.12
Strain at −45° (%)	0.07	0.02	-0.13	0.19	0.06	-0.27	0.28	-0.24	0.27	-0.27
Shear strain (%)	0.15	-0.07	-0.44	0.49	0.02	-0.45	0.79	0.61	0.47	0.39
Curvature at +45° (mm^{-1})	0.009	-0.06	0.025	-0.005	-0.002	0.007	0.001	0.009	-0.022	0.013
Curvature at −45° (mm^{-1})	-0.008	-0.059	0.007	0.001	0.002	0.022	0.004	0.055	-0.006	0.039
Twist (mm^{-1})	-0.018	-0.002	0.047	-0.006	-0.009	0.023	-0.007	0.045	-0.015	0.068

Table 2: Mid-plane strain and curvature components corresponding to critical locations of Figure 15

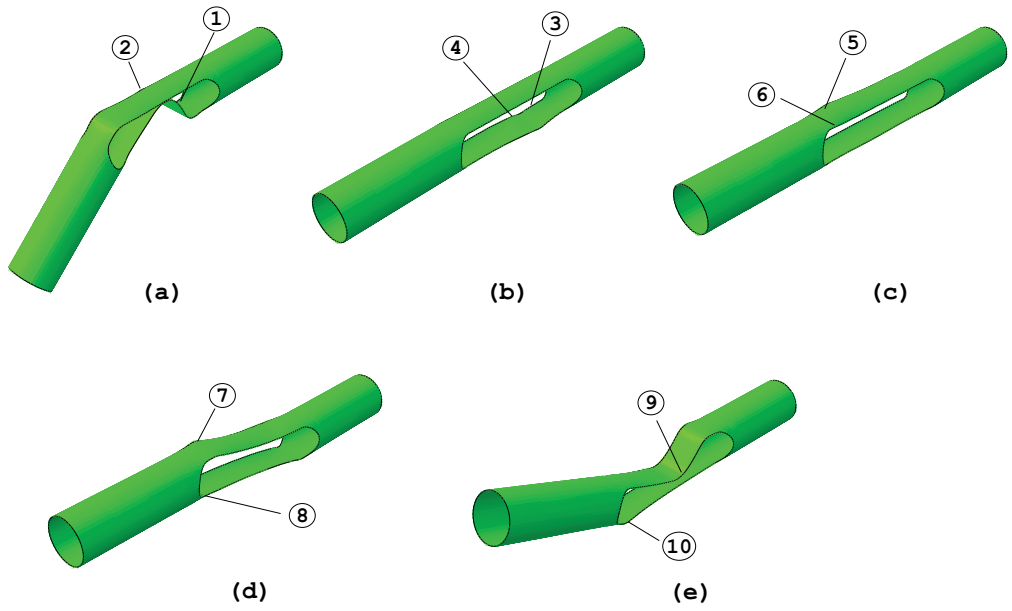

Figure 15: Critical regions from zero-gravity deployment simulation for hinge folded 45 deg; (a) fully folded (b) just before snap-back (c) snap-back (d) back buckling (e) maximum overshoot.

Location	1	2	3	4	5	6	7	8	9	10
Fibre strain (%)	0.42	0.71	0.13	0.32	0.26	-0.60	0.42	-0.94	0.61	0.13
Matrix strain (%)	0.92	1.6	0.23	0.70	0.52	-1.46	1.10	-2.00	1.30	-1.86

Table 3: Maximum strains at critical locations of Figure 15

T300 fibers are capable of carrying strains up to 1.5%[9] and hence the hinge is safe with a margin of 37% as far as fibre failure is concerned. However, the tensile failure strain of HexPly913 is around 1.93%[10] and hence locations 8 and 10 (where the matrix strains are however compressive) are potential failure regions. Note that these two locations are in the region of transition between a straight and a circular cut in the tube hinge; the vulnerability of these regions had been already identified.[5]

VI. Comparison of Simulations and Experiments

Figure 16 and Figure 17 compare the measured angle-time response with the predictions from zero-gravity and one-g simulations for booms with both 45 deg and 90 deg folds. In both cases there is excellent agreement between experiment and simulation during the initial deployment phase. For example, for the boom folded 45 deg the simulation showed a monotonic decrease in deployment angle from 45 deg to 0 deg over a period of 0.93 s; in the experiment it took 0.96 s. It is interesting to note that the inclusion of gravity and of the gravity offload cable has practically no effect on this initial deployment phase.

The second phase of the dynamic process shows some very interesting behaviour. The experimental angle-time relationship for the boom folded 45 deg, Figure 16, shows that this boom rotated 17 deg beyond the fully deployed configuration and became fully latched the second time it reached the fully deployed configuration. The angle-time relationships from the two simulations are different. The zero-gravity simulation predicts that the boom will go through the fully deployed configuration 4 times before becoming fully latched; on the other hand, the one-g simulation with gravity offload predicts that the boom will become fully latched on the first occasion. A detailed analysis of the sequence of configurations predicted by the two simulations, Figure 18, shows that the differences are relatively small (the images at 0.9 s appear identical) but in the one-g case there is alternate buckling without an overall motion developing. The net effect is that the hinge

remains latched. The sensitivity of these results indicates that the particular hinge design that has been selected for the present study is rather unpredictable.

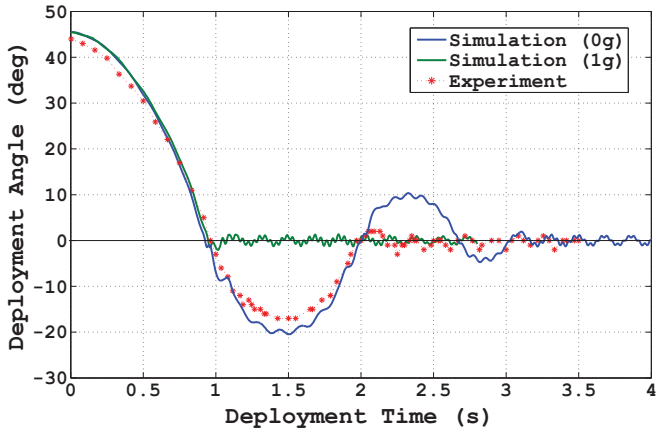

Figure 16: Comparison of experiment and simulation results for boom folded 45 deg.

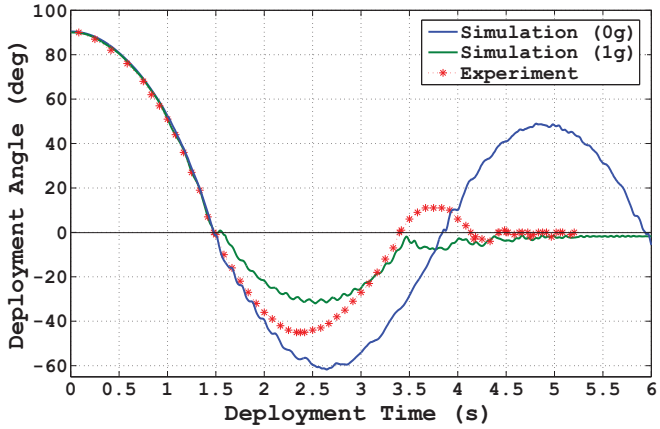

Figure 17: Comparison of experiment and simulation results for boom folded 90 deg.

The boom folded 90 deg shows a somewhat similarly unpredictable behaviour, but its sensitivity to small changes manifests itself during the second latching attempt. The one-g simulation of this boom shows that it started rotating backwards the second time it went through the fully-deployed configuration, whereas the zero-g simulation (as well as the experiment) shows that it went through this configuration.

Figure 19 compares a series of snapshots from simulation (in zero-g conditions) and experiment for a boom folded 90 deg. These images show that the present simulation technique is highly effective in capturing both overall and localized behaviour of the slotted hinge during deployment. It should be noted that even the images at the end of the selected sequence, at $t = 1.75$ s, show a similar deployment angle and also a very similar actual deformation of the tape springs.

VII. Conclusions

This paper has extended to deployment the work began in Refs.[4,5] The dynamic deployment behaviour of an integral slotted hinge made from a two-ply plain weave carbon fiber laminate has been studied both experimentally and by means of detailed finite-element simulations. A gravity compensation system was used for the experiments. The simulations, both with and without gravity effects, have allowed us to study the effects of the gravity offload system on the deployment behaviour.

The dynamic deployment behaviour of a boom with a slotted hinge can be divided into three phases, as

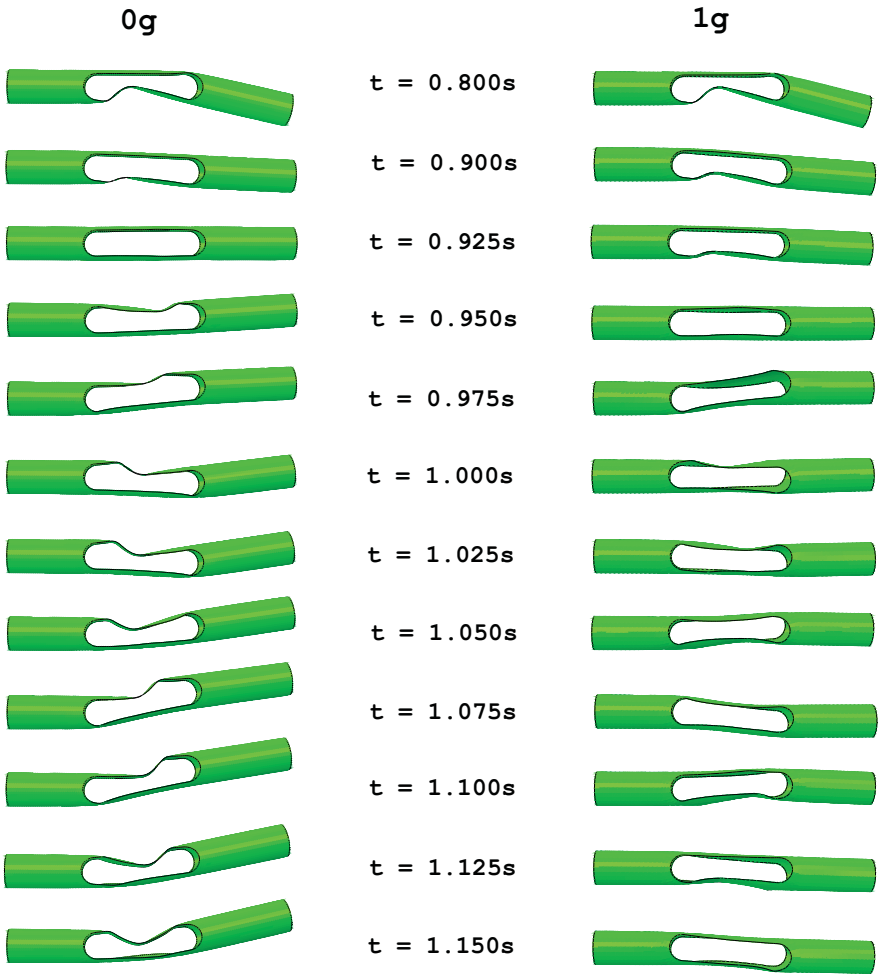

Figure 18: Snapshots near the fully deployed configuration from simulations with and without gravity effects, for boom folded 45 deg.

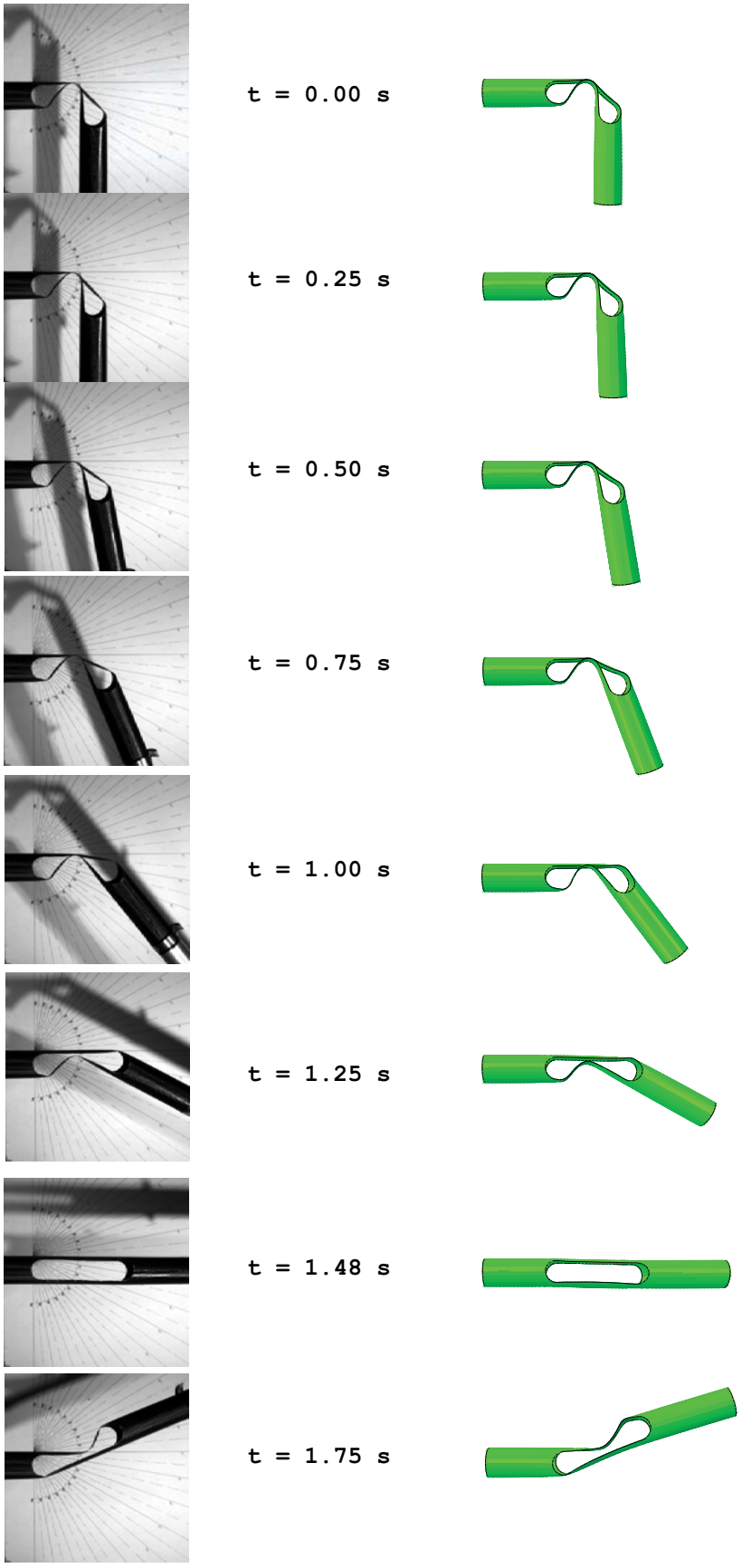

Figure 19: Snapshots from experiment and zero-gravity simulation (90 deg deployment).

follows:

1. deployment phase;

2. incomplete latching and large rotation phase;

3. vibration phase.

Our simulations have shown that the most critical phase is the second one, as the highest strains in both the fibres and the matrix occur at this stage. In fact, a detailed analysis of strains in the structure has shown that for the particular case of a boom folded 45 deg, the strains in the fully folded configuration are approximately 30% lower than the peak values.

It has been found that the presence of gravity effects and of a gravity offload system had significant effects on the incomplete latching and large rotation phase of the particular boom that has been investigated. It is thought that it may be possible to modify the hinge design in such a way that the boom deployment will be less sensitive to gravity, as it is highly desirable for practical applications that the deployment process should be insensitive to the gravity offload system.

In the next stage of this research the hinge configuration and the carbon-fibre laminate will be optimized with the aid of deployment simulations such as those presented in this paper. The simulations can also be used to identify critical configurations which would cause the structure to fail. It may be possible to avoid these critical configurations; for example the tube hinge considered is particularly vulnerable when the back tape spring buckles. These configurations could be avoided or the associated strains reduced by introducing damping mechanisms, limiting the folding angle or preventing tape spring buckling with a separate structure.

Acknowledgments

We thank Drs Ahmad Kueh, Julian Santiago Prowald and Michael Sutcliffe for helpful discussions. We are grateful to John Ellis (Hexcel, UK) for providing materials and Professor Chiara Daraio, Dr Alessandro Spadoni and Tian Lan for help with high speed imaging. HM thanks the Cambridge Commonwealth Trust and California Institute of Technology for financial support.

References

[1]Adams, D.S. and Mobrem, M. (2006) "MARSIS antenna flight deployment anomaly and resolution," *47th AIAA/ASME/ASCE/AHS/ASC Structures, Structural Dynamics, and Materials Conference*, AIAA 2006-1684 1 - 4 May 2006, Newport, Rhode Island.

[2]Boesch, C., Pereira, C., John, R., Schmidt, T., Seifart, K., Sparr, H., Lautier, J.M., Pyttel, T. (2008) "Ultra Light Self-Motorized Mechanism for Deployment of Light Weight Space Craft Appendages," *39th Proceedings of Aerospace Mechanisms Symposium*, 7-9 May 2008, Newport, NASA Marshall Space Flight Center.

[3]Yee, J.C.H. and Pellegrino, S. (2005) "Composite tube hinges," *Journal of Aerospace Engineering*, Vol. 18, No. 4, pp. 224–231.

[4]Mallikarachchi, H.M.Y.C. and Pellegrino, S. (2008) "Simulation of Quasi-Static Folding and Deployment of Ultra- Thin Composite Structures," *49th AIAA/ASME/ASCE/AHS/ASC Structures, Structural Dynamics, and Materials Conference*, AIAA-2008-2053, Schaumburg, Illinois, 07-10 April 2008.

[5]Mallikarachchi, H.M.Y.C. and Pellegrino, S. (2009) "Simulation of Quasi- Static Folding and Deployment of Ultra- Thin Composite Structures," submitted for publication.

[6]SIMULIA, ABAQUS/Explicit Version 6.7, Providence, RI.

[7]Kueh, A.B.H. and Pellegrino, S. (2007) "ABD matrix of single-ply triaxial weave fabric composites," *48th AIAA/ASME/ASCE/AHS/ASC Structures, Structural Dynamics, and Materials Conference*, AIAA-2007-2161, Honolulu, Hawaii, 23-26 April 2007.

[8]Belytschko, T., Liu, W.K. and Moran, B. (2000) 6.2.3 Energy balance, *Nonlinear Finite Elements for Continua and Structures,* Chichester, J. Wiley & Sons. , pp. 315-316.

[9]Torayca. Technical Data Sheet No. CFA-001, T300 Data Sheet.

[10]Hexcel Corporation. Technical Data Sheet HexPly913, 2007.